Available online at www.sciencedirect.com

ScienceDirect

Procedia CIRP 137 (2025) 217–222

www.elsevier.com/locate/procedia

CIRP Conference on Electro Physical and Chemical Engineering

Penetration Detection for Small-Hole Drilling EDM Based on LSTM

Zhao yehuan[a],Liu jianyong[a,*],Liu fangyuan [a],Luo xueke [a],Xu mingcheng [a]

[a]*Beijing Institute Of Petrochemical Technology, No. 19 Qingyuan North Road Daxing District, Beijing City and 102617,China*

* Corresponding author. Tel.: +86-18611404035; fax: +86-18611404035. *E-mail address:* ljy_18778@163.com

Abstract

To address the problem of complex discharge state changes during perforation in EDM small-hole drilling, which result in untimely detection and low accuracy, this paper proposes a state monitoring method that integrates Long Short-Term Memory (LSTM) networks with machining parameters. First, the processing depth, speed, current, and voltage signals are normalized to achieve feature dimensionality reduction. Then, a state prediction model is constructed using a Long Short-Term Memory (LSTM) network, enabling the prediction of the current-stage data's state value based on historical machining data. Finally, the perforation state of small-hole machining is determined by comparing the measured and predicted values. The input of the model includes machining depth, speed and machining current, and the output is whether penetration occurs. A penetration detection platform was established to validate the proposed method. The measured data indicate that the penetration recognition rate for 200 holes reaches 96%, and the minimum penetration distance is maintained below 0.5mm. Therefore, this method can achieve effective penetration monitoring in small-hole EDM machining, and it exhibits good model stability and accuracy.

Keywords: EDM small-hole drilling, machining parameters, penetration detection, LSTM;

1. Introduction

EDM small-hole machining is a key technology in the field of special machining, and it is a non-contact process [1]. This technology offers advantages such as no cutting force, high processing accuracy, and a large depth-to-diameter ratio. By controlling the pulse power and output power, it can meet the process requirements for precision manufacturing. However, in the actual process of small-hole EDM, not only will the workpiece undergo electro-erosion, but the tool electrode will also experience wear due to the discharge energy of EDM. Due to this phenomenon, the method of given depth machining is currently commonly used, but it is only suitable for situations where the processing accuracy is not high. For machining with high precision requirements, such as the air-film cooling holes in turbine blades [2], traditional methods often lead to issues such as non-conformance of the hole diameter on the back of the workpiece and damage to the workpiece. Therefore, effective penetration detection is critical to improving the efficiency and quality of EDM small-hole machining.

When utilizing electrical discharge micro-drilling technology, accurately determining the precise moment of tool electrode penetration has emerged as a significant challenge for achieving high-precision processing. Presently, numerous scholars both domestically and internationally have dedicated their efforts to researching this issue. Lin et al. utilized the high-frequency spectrum of the gap voltage for penetration detection [3]. Koshy et al. developed a method based on pneumatic measurement principles to determine whether penetration has occurred by analyzing the internal flushing pressure within the electrode and its position [4]. Zhu Yunbin et al. developed a method for penetration detection by statistically analyzing the frequency of voltage fluctuations through voltage monitoring and comparing the results with a predefined threshold [5]. Cheol-Soo Lee et al. [6] established a mathematical model of tool electrode wear and experimentally analyzed the relationship between wear rate and processing time. Using this

10.1016/j.procir.2025.03.074

model, they predicted the electrode wear rate for subsequent processing stages and determined the actual position of the tool electrode by incorporating the preset processing depth, thereby enabling accurate detection of penetration. Peng Jiarong [7]developed a penetration detection method by comparing the feed rate before and after the occurrence of penetration.

Xia W et al [8]selected the effective discharge frequency and electrode feed speed as the characteristic quantities for penetration detection and applied them to the support vector classification (SVC) model based on the radial basis kernel function. After training, this model accurately identified the instant of small-hole penetration. Zhu Y [9] accurately determined the occurrence of penetration by analyzing the changes in the flow field within the processing gap before and after penetration, and comparing the voltage, voltage change rate, and current values against the predefined threshold values. Shi D et al [10] utilized the average voltage detection method to determine the processing voltage. To prevent misjudgment caused by transient short circuits and open circuits during the processing phase, they implemented a technique involving the collection of several hundred consecutive voltage readings and calculating their mean value. This mean voltage was then compared with the threshold voltage of 0.3V, which was established through waveform analysis. If the mean voltage fell below this threshold, it was classified as penetration. Bai K et al [11] analyzed the wear of the tool electrode during small-hole machining and investigated the influence of various factors using an orthogonal experimental design, subsequently ranking these factors. The results indicated that the most significant factors, in order of importance, were peak processing current, workpiece thickness, flushing pressure, and pulse interval and width. Based on a radial basis function (RBF) network, they developed a corresponding predictive model. Experimental validation demonstrated that the prediction error of this model was within 9%. Wang Z et al [12] observed that no electric sparks appear on the backside of a machined workpiece before penetration, while spark activity increases upon penetration. Photosensitive sensors captured light signals transmitted by diodes fixed beneath the workpiece. These signals were converted to electrical signals and transmitted to a control chip, where comparisons with preset values enabled penetration detection. Wang J et al [13] selected pulse width, pulse interval, average gap current, and electrode feed rate as characteristic parameters for processing status, with the classification output indicating whether penetration occurred. They employed four machine learning algorithms to conduct offline training and online testing on these characteristic parameters. Ultimately, the penetration detection model built based on a radial basis function support vector machine (RBF-SVM) performed the best. Xia W [14] analyzed the significant fluctuations in the conditional no-load rate before and after penetration and subsequently established a threshold of 0.95 for the conditional no-load rate to determine the occurrence of penetration. Xie W[15] utilized the wavelet transform method to perform high-precision real-time monitoring of the discharge state during the electrical discharge machining process, thereby significantly enhancing the efficiency and stability of micro-electrical discharge machining. Wang J[16] conducted efficient processing of diffuser-type film cooling holes by employing a hybrid method that combines high-speed electric discharge drilling and milling on an electric discharge drilling machine equipped with tubular electrodes and high-pressure internal cooling. Through range analysis method, the processing efficiency of the diffuser type film cooling holes was improved. Zhang H et al [17] proposed a penetration detection technology for electrical discharge micro-hole machining based on the BP neural network classification algorithm in response to the issue that the loss of the electrode itself affects the electrical discharge micro-hole machining. Wang J [18] developed a penetration detection classification model in MATLAB by iteratively training and learning from the experimental data of processing voltage using the BP neural network classification algorithm.

With the development and application of intelligent technologies, many experts and scholars have applied technologies such as BP neural network models, support vector machines, and random forests to the penetration detection of electrical discharge micro-drilling. Using these techniques, they have developed predictive models for penetration detection in electrical discharge micro-drilling and achieved relatively good prediction performance. Currently, all machine learning methods employed in the penetration detection of electrical discharge micro-hole machining are shallow learning methods [19]. These methods exhibit limited capability in fitting complex functions, resulting in poor engineering applicability. In actual complex processing scenarios, these methods still suffer from issues such as untimely recognition of penetration signals and low penetration detection efficiency. The "depth" of deep learning effectively addresses the limitations of shallow learning methods. However, deep learning network models are typically more complex, incorporating multiple hidden layers. Consequently, these models exhibit superior feature representation capabilities, enhanced function approximation abilities, and improved generalization performance. Secondly, the parameters of the network model are obtained through training with a large amount of sample data, and the feature extraction of the model is achieved through autonomous learning, eliminating the need to rely on human experience. To address the urgent need for real-time penetration detection under complex working conditions, this paper proposes a penetration detection method based on Long Short-Term Memory (LSTM) and dimensionality reduction of multiple machining parameters, building upon previous research. This method comprehensively considers signals such as depth, speed, current, and voltage during the machining process to construct a state model that can predict parameter values at the next moment. By calculating the difference between actual measured values and LSTM-predicted values and comparing them with self-learned state thresholds, the machining status is determined. Finally, the effectiveness and accuracy of this method are validated using experimental data.

2. System Architecture Design for LSTM Modeling

LSTM networks are a specialized form of Recurrent Neural Networks (RNNs). To address the two major drawbacks of RNNs, namely gradient vanishing and gradient explosion, as well as the inability to capture long-term dependencies in

sequences, LSTM networks were developed. The key feature of LSTM is its ability to learn long-range dependencies. LSTM networks were first proposed by Hochreiter and Schmidhuber in 1997 and have since been refined by many researchers [20]. They have demonstrated strong performance across various problems and are now widely utilized. The basic structure of the LSTM network comprises input gates, output gates, and forget gates. These components enable the network to retain essential information from the original data, thereby achieving effective memory function. The cell structure of the hidden layer in the LSTM network is illustrated in Fig. 1.

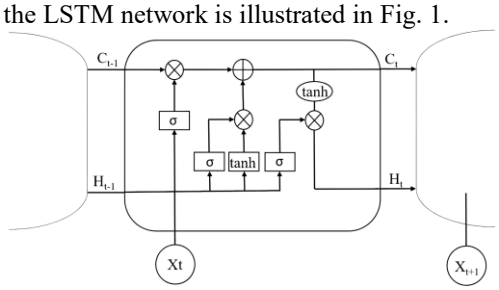

Fig. 1 LSTM hidden layer cell structure.

In the LSTM network, X_t and H_t represent the input vector and the hidden state of the LSTM unit at time t, respectively. The sigmoid activation function and hyperbolic tangent activation function are denoted by σ() and tanh, respectively. $\oplus$ denotes element-wise addition, and $\otimes$ denotes element-wise multiplication. The algorithm model can add or remove information from the states of each unit through its gate structures [21].

(1) The forget gate [22] : the forget gate determines which information from the previous time step's unit state needs to be forgotten, that is, how much information is retained to the current moment 0.The hidden state of the previous moment and the input information of the current moment are passed to the sigmoid function, and the output value is between 0 and 1, the closer to 1 means that the information should be retained, conversely, it should be forgotten. Its calculation method is as shown in Eq. (1).

$$f_t = \sigma(W_f[h_{t-1}, x_t] + b_f) \tag{1}$$

Where h_{t-1} is the hidden state information from the previous time step, b_f and W_f are the bias and weight vectors of the forget gate, respectively.

(2) The input gate: the update of the unit state at the current moment is completed by the input gate. Firstly, the input information of the current moment and the hidden state of the previous moment are input to the tanh function and sigmoid function respectively, the sigmoid function determines the information that needs to be retained, and the tanh function generates the candidate vectors, and the computation process is respectively shown in Eq. (2) to (3); then i_t and g_t are multiplied point by point as the information that needs to be newly added to the unit state, and finally Add it with the output of the forgetting gate point by point to complete the update of the unit state, the process is shown in Eq. (4).

$$i_t = \sigma(W_i[h_{t-1}, x_t] + b_i) \tag{2}$$

$$g_t = tanh(W_g[h_{t-1}, x_t] + b_g) \tag{3}$$

$$C_t = f_t C_{t-1} + i_t g_t \tag{4}$$

In the formula: W_i and b_i represent respectively the weight vectors and bias of the implicit layer with sigmoid activation function in the input gate; W_g and b_g are respectively the weight vectors and bias of the hidden layer with the activation function of tanh in the input gate.

(3) The output gate: the hidden state value at the current moment is determined by the output gate. Firstly, the hidden state of the previous moment and the input information of the current moment are passed to the sigmoid function, and then the cell state of the current moment is passed to the tanh function, and finally the outputs of sigmoid and tanh are multiplied point by point to get the hidden state value, and the process is as shown in Eq. (5).

$$o_t = \sigma(W_o[h_{t-1}, x_t] + b_o) \;\; h_t = o_t tanh C_t \tag{5}$$

In the formula: W_o and b_o respectively represent the weight vector and bias of the hidden layer in the output gate.

3. Constructing an LSTM penetration detection model

During the moment of penetration and the complete penetration process in electrical discharge micro-hole machining, the processing current will increase rapidly, while the processing voltage will drop rapidly, approaching a short-circuit state. At the same time, the processing speed slows down. The processing states before and after the penetration in electrical discharge micro-hole machining are shown in Fig 2.

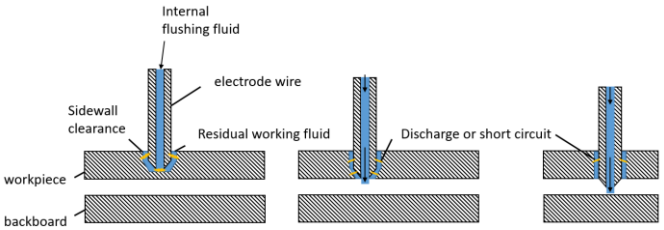

Fig. 2. (a) Before penetration; (b) At the moment of penetration; (c) After penetration.

The proposed method employs depth, speed, current, and voltage parameters to monitor the state of electrical discharge micro-drilling [23]. A prediction model and reference threshold are established based on normal-state data. The system then compares the differences between the predicted results and the measured data to assess the condition of the electrical discharge machining process. The monitoring procedure is illustrated in Fig. 3.

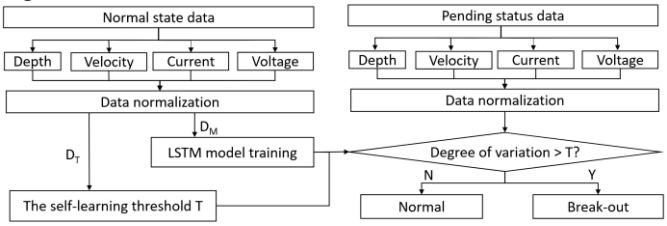

Fig. 3 Monitoring methodology flow.

3.1. Test data collection

The equipment used for the experiments in this paper is AREDM-H30 six-axis EDM small-hole machining machine, as shown in Fig. 4. The Computer Numerical Control (CNC) system of this machine uses a dual-core 'Windows+RTX' architecture, which handles real-time and non-real-time tasks separately. The effectiveness of this system structure has been validated through the machining of a space engine turbine disk [24].

Fig. 4 AREDM-H30 6-axis EDM machine for small-hole machining.

In this paper, a total of eight specifications of brass electrode wires with diameters ranging from 0.3 to 1 mm will be used to conduct penetration tests on 304 stainless steel materials with different thicknesses (0.5, 1, 3, 5, 10 and 20 mm), respectively. Using the same set of machining process parameters [25], the test was divided into 48 groups, and each group was continuously machined 50 holes.

During the stable operation phase of EDM, depth, speed, current, and voltage data are collected. Depth signals are obtained from the positional changes of the W-axis, which is the machining axis where the electrode is located. Speed signals are derived from the rate of positional change of the W-axis per second. Current and voltage signals are acquired from the voltage and current values between the electrode and the workpiece using a high-frequency acquisition device. During the drilling process, the numerical control (NC) system records the time-series data for depth, speed, current, and voltage. After processing is completed, these values are stored in corresponding .xls files. A total of 2400 holes were drilled, with each group consisting of 48 documents. Each document records the changes in the four characteristic parameters of 50 holes at different processing times under identical conditions. Selected records are shown in Figure 5. The figure illustrates the temporal variations in depth speed, current, and voltage during the small hole machining process. Specifically, the depth speed is updated once per second, whereas the current and voltage data are recorded at intervals of 0.125 seconds.

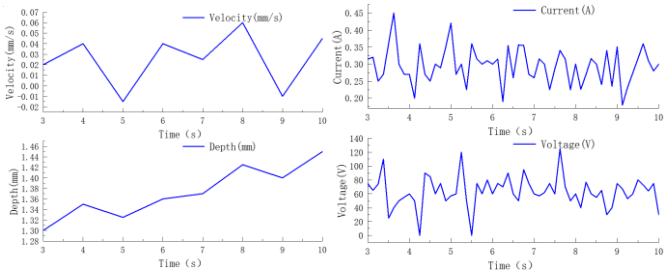

Fig. 5 CNC small-hole machining process feature quantity recording interface.

After removing the invalid parameters of holes that do not meet the standards, the feature values recorded during the machining process of the remaining 2,000 conforming holes will be used as the sample set for the model.

3.2. Modeling

The current, voltage, depth, and speed signals collected during the machining process are used as feature vectors, which have different units and large numerical discrepancies. Therefore, it is necessary to normalize these signals, constraining the normalized feature data within the range of [0,1] to meet the input requirements of the LSTM model.

The calculation formula for normalizing processing data is shown in Eq. (6).

$$X_i^* = \frac{X - X_{min}}{X_{max} - X_{min}} \tag{6}$$

Where X is the actual value, X_i^* is the result value after normalization of the actual value, X_{max} is the maximum value of the characteristic factors, X_{min} is the minimum value of the characteristic factors.

The LSTM model is employed to process the four parameters of EDM micro-hole machining as a sequential problem. Through training at the previous time step, the internal state information of each machining parameter is extracted via the network structure and passed to the subsequent time step. This process influences the target output at the next time step, enabling it to better reflect the coordination relationship among machining parameters.

In this paper, the LSTM-based penetration detection model for EDM small-hole machining is constructed using Python and the TensorFlow framework. The model consists of an input layer, an LSTM layer, a Dropout layer, a fully connected layer, and an output layer. The algorithm flow of the model is illustrated in Fig. 6.

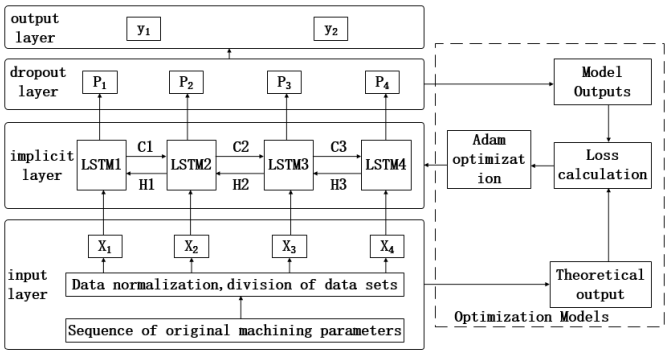

Fig. 6 Algorithm flowchart of the penetration detection model.

The input layer of the penetration detection model shown in Figure 6 contains four factors: depth, speed, current, and voltage. The implicit layer consist of four LSTM cell layers, denoted as LSTMi (i = 1, 2, 3, 4), where the number of cell units in the first layer is 128, in the second layer is 64, in the third layer is 32, and in the fourth layer is 16. The Dropout layer is used to prevent overfitting during the training of the network model. The fully connected layer maps the learned features to

the specific output categories. And the output layer has two output targets: whether the processing is penetrating or not.

The proposed method sets the objective function of the state monitoring model as shown in Eq. (7), which can be minimized using the Adam (Adaptive Moment Estimation) optimization algorithm J. This optimization algorithm uses the first- and second-order moment estimates of the gradient to dynamically adjust the learning rate for each parameter, ensuring a well-defined learning rate range for each iteration. This results in smooth parameter updates and reduces the model's learning time.

$$\mathrm{J} = \frac{1}{2\times N}\sum_{t=1}^{N}(h(F_t) - F_{rt})^2 \tag{7}$$

Where: $h(F_t)$is the predicted value of the prediction model for the input data F_t, F_{rt} is the measured value.

The training of the state monitoring model and threshold self-learning based on the normalized dataset D are performed as follows.

3.3. State detection model training

Through data collection, 2,000 sets of valid sample data were obtained, with 70% randomly selected as the training sample set and 30% as the test sample set. The first 1,000 groups of the training sample set are used to train the network model, while the last 400 groups are used for self-learning the penetration threshold. The number of training sessions is set to 300 to balance computational efficiency and achieve a small loss function value.

3.4. Threshold self-learning

When an abnormal change in the EDM processing state occurs, it is accompanied by changes in multiple feature values. To accurately represent the differences in multi-dimensional features and maximize these differences, the Mahalanobis distance is selected to measure the degree of discrepancy between the measured and predicted values. The 3σ criterion is used to set the monitoring threshold, and the absolute value of the difference between the measured value and the predicted value in self-learning threshold data (D_T) is shown in Eq. (8).

$$\Delta\mathrm{F} = \{\Delta f_t\} = \{|h(F_t) - F_{rt}|\} \;\; t \in [N+1, M] \tag{8}$$

Where$\Delta f_t$is the difference vector between the true values and predicted values, with a dimension of H. The Mahalanobis distance between each element of $\Delta\mathrm{F}$ and the mean value $\overline{f_t}$ of $\Delta\mathrm{F}$ forms the set shown in Eq. (9).

$$\mathrm{y}(\Delta f_t) = \sqrt{(\Delta f_t - \overline{f_t})\Sigma^{-1}(\Delta f_t - \overline{f_t})^T}$$

$$F_e = f(\Delta f_t) \;\; t \in [N+1, M] \tag{9}$$

Sorting the elements within F_e in ascending order, taking the upper quartile of F_e as Q_2 and the lower quartile as Q_1,the state monitoring threshold is shown in Eq. (10).

$$\mathrm{T} = Q_2 + 1.5 \times (Q_2 - Q_1) \tag{10}$$

After completing the training, the same state features as those in the training data of the state monitoring model are extracted for a randomly selected test sample set. The processing state is then determined to be either 'normal' or 'penetration' based on whether the discrepancy between the measured and predicted values exceeds the monitoring threshold.

4. Experiment verification

The self-developed penetration detection module is integrated into the EDM numerical control system, with current and voltage sensors selected to collect the signals. Improve the accuracy of discharge state detection through timed sampling of the processing state. By establishing a discharge state monitoring interface, the processing depth, speed, current, and voltage can be monitored in real time. The platform facilitates the acquisition and analysis of processing voltage and current signals, delivers timely feedback on penetration status information to the machine tool, and manages the processing workflow. The overall structure of the platform program is illustrated in Fig. 7.

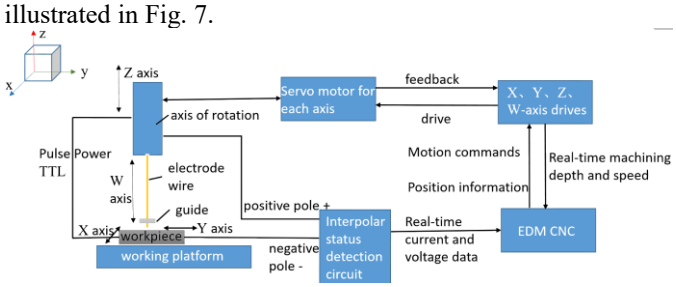

Fig.7 Overall scheme of EDM penetration detection.

According to the overall scheme of the composite machining penetration detection platform shown in Fig. 7, the platform is divided into three parts:

(1) The EDM penetration detection data acquisition system is primarily responsible for the real-time acquisition of machining voltage, current, depth, and speed signals.

(2) Machining state analysis is performed based on the LSTM network, and programming algorithms are developed to implement the principle of machining penetration detection

(3) The penetration signal output circuit and the machine tool control system are responsible for controlling the tool lift of the machine tool spindle after detection of penetration.

EDM micro-hole machining experiments were conducted based on the proposed penetration detection technique. The validation process involved 10 groups, with each group consisting of 20 consecutive holes. The final penetration detection accuracy reaches 96%, and the minimum downward movement distance of the electrode wire after penetration is controlled within 0.5 mm. The actual processed double-layer sample and hole configuration are illustrated in Figure 8.

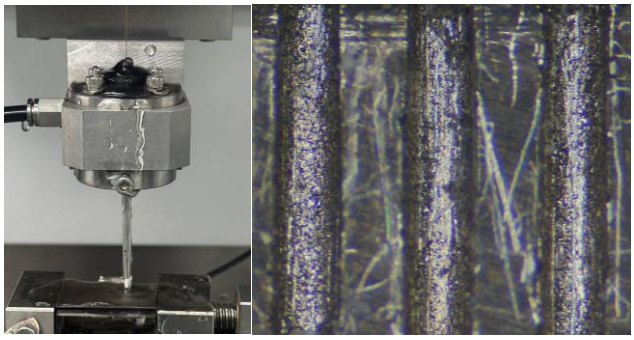

Fig. 8. (a) Diagram of actual machining workpiece; (b) Cross-sectional view of the processed hole.

5. Conclusion

In this paper, a penetration detection method based on LSTM for EDM small-hole machining is proposed and studied. The method is analyzed and verified through punching experiments, and the following conclusions are drawn.

The LSTM-based EDM penetration detection technology can accurately identify the moment of electrode penetration, enabling the electrode to promptly stop processing and back off. Furthermore, the depth at the moment of penetration is recorded before each back-off. This technology is applicable to workpieces of varying thicknesses.

By using depth, speed, current, and voltage as monitoring parameters to identify the moment of penetration during small-hole machining, the penetration recognition accuracy reaches 96%. This detection technology demonstrates exceptionally high reliability.

The minimum displacement of the electrode wire after penetration is controlled within 0.5 mm. When applied to the machining of air-film holes in aerospace blades, this technology can effectively prevent damage to the backside of the blades, demonstrating strong practical applicability.

Although the experimental results demonstrate that the proposed LSTM-based penetration detection method for EDM small hole machining holds significant potential, this paper presents only preliminary findings. The method has been developed in a controlled experimental environment and requires further in-depth research before it can be applied to industrial production. Future studies should consider integrating frequency domain feature analysis with the time domain feature analysis conducted in this study to enhance the accuracy of online penetration detection. Additionally, as artificial intelligence technology advances, mature AI models can be applied to EDM small hole machining penetration detection to achieve adaptive penetration detection capabilities.

Acknowledgements

This work was sponsored by Beijing Nova Program (No. 20240484626,20230484429).

References

[1] Jiang Y. Research on process control system of micro-hole EDM. Shanghai: Shanghai Jiao Tong University; 2011.

[2] Ji R, Liu Y, Zhang Y, Wang F. Machining performance of silicon carbide ceramic in end electric discharge milling. International Journal of Refractory Metals and Hard Materials 2011;29(1): 117-122.

[3] Lin J K, Nien Y F. Automatic breakthrough detection device: US6723942 B1 ;2003-03-06.

[4] Koshy P, Boroumand M, Ziada Y. Breakout detection in fast hole electrical discharge machining. International Journal of Machine Tools and Manufacture 2010;50(10):922-925.

[5] Zhu Y B, Li T J. A penetration detection method of an electric spark perforator: 201310398374.9; 2013-12-18.

[6] Lee C S, Heo E Y, Kim J M, et al. Electrode wear estimation model for EDM drilling. Robotics and computer Integrated Manufacturing 2015; 36:70-75.

[7] Peng J. Breakdown recognition system and recognition method for electrical discharge drilling machine 201510677813.9; 2016-01-13.

[8] Xia W, Wang J Q, Zhao W S. Break-out detection for high-speed small hole drilling EDM based on machine learning. Procedia CIRP 68 (2018) 569 – 574.

[9] Zhu Y. Penetration detection and experimental research on micro-hole EDM-electrolytic composite machining. Nanjing: Nanjing University of Aeronautics and Astronautics; 2016.

[10] Shi D. Research on electrical discharge machining process and penetration detection technology for micro-holes in high tungsten alloy. Harbin Institute of Technology; 2017.

[11] Bai J, Hu H, Guo Y. Research on electrode loss prediction technology for high-speed EDM small hole machining. Proceedings of the Annual Conference of the Chinese Mechanical Engineering Society; 2007.

[12] Wang Z, Li S. Design of Through-Hole Detection Device for Electrical Discharge Drilling Machine Based on 51 Single-Chip Microcomputer. Techniques of automation and applications 2019; 38:168-171.

[13] Wang J, Xia W, Xi X, et al. Performance comparison of several machine learning algorithms in small hole EDM penetration detection. Proceedings of the 18th National Academic Conference on Special Machining (Abstract). Urumqi:Special Machining Branch of Chinese Mechanical Engineering Society; 2019.

[14] Xia W. Penetration detection and adaptive control for high-speed EDM of small holes. Shanghai Jiao Tong University; 2020.

[15] Xie W, Zhang T, Yang X. Study on discharge state detection of micro-EDM based on wavelet transform method. Procedia CIRP 113 (2022) 70–74.

[16] Wang J, Gao Q, Xi X, et al. Experimental study of EDM milling of 3D-shaped diffuser for film cooling holes on turbine blades. Procedia CIRP 113 (2022) 160–165.

[17] Zhang H, Wang J, Liang L, et al. Research on penetration detection technology of EDM small hole machining based on BP neuron algorithm. Electro machining and Mold 2023;03:14-19.

[18] Wang J. Research on penetration detection control technology of EDM small hole machine based on classification algorithm. North University of Technology; 2023.

[19] Wang M, Gao X, Liu J. Performance prediction of EDM small hole machining process target based on LSTM recurrent neural network[J]. Modern Manufacturing Engineering 2020;12:75-82.

[20] Wang X, Wu J, Liu C, et al. Fault time series prediction based on LSTM recurrent neural network. Journal of Beijing University of Aeronautics and Astronautics 2018;44(4):772-784.

[21] Shi Y, Li Q, Xiong H. Rate-constrained traffic prediction for TTE networks based on LSTM. Journal of Beijing University of Aeronautics and Astronautics 2020;46(4):822-829.

[22] Zheng B, Jin H, Meng Y, et al. Improved LSTM for early warning and optimization of denitrification in coal-fired power plants. Energy conservation and environmental protection 2021;2(8):53-60.

[23] Ji R, Zhao Q, Zhao L, et al. Study on high wear resistance surface texture of electrical discharge machining based on a new water-in-oil working fluid. Tribology International, 2023, 180: 108218.

[24] Luo X, Liu J, Liu J,et al. Development of a Modular Six-Axis Electrical Discharge Micro-Hole Machine Numerical Control System. Electromachining & Mould 2023;04:13-19.

[25] Ji R, Liu Y Zhang Y, et al. Influence of dielectric and machining parameters on the process performance for electric discharge milling of SiC ceramic. The International Journal of Advanced Manufacturing Technology. 2012, 59: 127-136.